Organic/Inorganic Hybrid of Polyaniline/$BaTiO_3$ Composites and Their Electrorheological and Dielectric Characteristics

Fei Fei Fang,[1] Ji Hye Kim,[1] Hyoung Jin Choi,[1] Yongsok Seo[2]

[1]*Department of Polymer Science and Engineering, Inha University, Incheon 402-751, Korea*
[2]*School of Materials Science and Engineering, Seoul National University, Seoul 151-744, Korea*

Received 29 December 2006; accepted 14 February 2007
DOI 10.1002/app.26359
Published online 26 April 2007 in Wiley InterScience (www.interscience.wiley.com).

ABSTRACT: Barium titanate ($BaTiO_3$) inorganic particles which possess large electronic resistance and excellent dielectric properties were employed to synthesize conducting polyaniline (PANI)/$BaTiO_3$ composites via an *in situ* oxidative polymerization, since conducting PANI/inorganic composites have been considered as a superior candidate of electrorheological (ER) fluids because of their physical properties, unique structure, and the combined merits of the two phases. The influence of the fraction of $BaTiO_3$ particles in the as-synthesized composites on the physical properties (morphology and crystal structure) and the ER behaviors were examined. Yield stress data obtained were analyzed based on the universal yield stress equation as a function of applied electric field and it was found that the universal yield stress equation collapses these data onto a single curve independent of $BaTiO_3$ particle concentration. Their shear stresses under an applied electric field were also found to be fitted well with the Cho–Choi–Jhon model. In addition, the investigated dielectric spectra were found to be useful to interpret the differences in the ER performances for the PANI/$BaTiO_3$ composite based ER fluids. © 2007 Wiley Periodicals, Inc. J Appl Polym Sci 105: 1853–1860, 2007

Key words: electrorheological fluid; dielectric; cole–cole plot; yield stress

INTRODUCTION

Electrorheological (ER) fluids, typically composed of polarizable particles dispersed in insulating liquid, are a kind of fascinating smart and intelligent material that can change the state reversibly within milliseconds with the aid of electric field.[1] Both structure and rheological properties (yield stress, shear viscosity, shear modulus, etc.) of the fluids are also changed dramatically.[2] Because of this unique variation of the rheological properties, the ER fluids have great potential applications in designing torque transducer, damper, actuator, and other control systems.[3,4] However, compared with the magnetorheological (MR) fluids which have achieved much commercial success in the industries,[5,6] the ER fluids still lack of obtaining widespread applications because of the low yield stress. Therefore, many researchers are focusing on developing novel ER materials possessing excellent ER behaviors. It is well known that all ER materials can be divided into both hydrous and anhydrous systems. For the former category, the modified starch or silica gel are typical instances, which generate better ER effect because of the enhanced polarizability from the water or some other polar molecule as an additive or promoter.[7–9] However, these hydrous ER particles have severe limitations in engineering application because of the poor thermal instability, ease of water evaporation as well as the corrosion of devices and so on. The latter type, also named as intrinsic ER systems, usually consists of semiconducting polymers or inorganic materials which overcome the above problem and represent excellent ER performances.[10–15] Furthermore, hybrid organic–inorganic composite based ER materials have gained increasing attentions because they can possess synergistic characteristics. They include polymer/clay nanocomposites, core/shell structured materials, polymer/mesoporous materials, and polymer/inorganic particles. We have explored many novel anhydrous ER systems and investigated the ER behaviors based on these semiconducting polymers, demonstrating a valuable scaling function for yield stress as a function of electric field strength which incorporates both the polarization and conduction models.[16] When mentioned to the yield stress, it is worthy to note that a novel ''giant electrorheological effect'' system with extremely high yield stress which was attributed to the proposed saturation surface polarization in the contact region of the neighboring spheres has been recently reported.[17]

Correspondence to: H. J. Choi (hjchoi@inha.ac.kr).
Contract grant sponsor: KOSEF; contract grant number: R01-2006-000-10,062-0.

Journal of Applied Polymer Science, Vol. 105, 1853–1860 (2007)

Meanwhile the interfacial polarization takes dominant role in determining the ER performances.[18,19] Thus, it is necessary to study the dielectric behaviors of the ER materials when analyzing the ER activity using this interfacial polarization theory. Many researches on the dielectric properties (dielectric constant and dielectric loss factor) have been reported.[20–23] Wang et al.[24] demonstrated that higher dielectric constant of the spheres lead to a stronger interaction force which was associated with the ER effect. Nevertheless, Hao et al.[25] proposed that a large dielectric loss factor which can give a large interfacial polarization was required for an ideal ER system.

Among various conducting polymers, the PANI is known to be one of the most attractive one because of several advantages such as high conductivity, stability, and easy synthesis in large quantities. In addition, inorganic nanoparticles can be introduced into the matrix of a host-conducting polymer, either by chemical methods or by electrochemical synthesis. Considering that ER effect of the electro-responsive particles could be enhanced by modifying the surface with highly polarizable semiconducting polymer, we synthesized conducting PANI/inorganic $BaTiO_3$ composites and examined the ER performances for PANI/$BaTiO_3$ composite with different fraction of $BaTiO_3$ (10 and 25 wt %) as a continuation of our previous work on the same system.[26,27] Even though this system has been recently investigated, its better understanding on ER performance still requires further investigation.[28,29] Here, we focused on investigating rheological and dielectric properties for the two ER fluids prepared using universal yield stress equation and rheological equation of state of Cho–Choi–Jhon (CCJ) model, and successfully interpreted the influence of the amount of inorganic $BaTiO_3$ particles on the ER behaviors using Cole–Cole plot.

EXPERIMENTAL

The PANI/$BaTiO_3$ hybrid composite was synthesized by an *in situ* chemical oxidation polymerization of aniline in the presence of $BaTiO_3$ nanoparticles (Inframat Advanced Materials, LLC, USA). At first, $BaTiO_3$ nanoparticles were dispersed in 450 mL of 1*M* HCl to get a homogeneous phase of solution by vigorous stirring at 0°C. After that, aniline monomer was added to this dispersion of $BaTiO_3$. Prechilled ammonium peroxysulfate (initiator) which was dissolved in 350 mL of 1*M* HCl in another beaker at 0°C was dropped into the above prepared dispersing phase within 4 h. After dropping the initiator, the mixture was kept stirring at 200 rpm at 0°C for 24 h. Then, the synthesized PANI/$BaTiO_3$ composites were centrifuged and filtered with distilled water, acetone, and methanol to remove excess initiator, monomer, and oligomers, and dried at 65°C in vacuum oven for 2 days. Two different fraction of $BaTiO_3$ nanoparticles (10 and 25 wt %) in the PANI/$BaTiO_3$ composites were prepared.

Since the above synthesized PANI/$BaTiO_3$ composites have so high conductivity, its direct ER test can not be carried out. Therefore, to apply for the ER test, we have to adjust the conductivity of the composite to an appropriate value via a dedoping process. We dispersed the synthesized PANI/$BaTiO_3$ composites in 1*M* NaOH solution and controlled the pH value to be 9 by adding either 1*M* NaOH or 1*M* HCl solution.[30] The product was then filtered, dried, and sieved. The conductivity was found to decrease from 2.41×10^{-1} to 1.67×10^{-12} S/cm and 8.13×10^{-12} S/cm for 10 and 25 wt % of PANI/$BaTiO_3$ composites separately.

FTIR spectroscopy (Perkin–Elmer System 2000) was used to examine the chemical structure of the composite prepared by grinding it with KBr. Thermal properties of PANI/$BaTiO_3$ composite were examined by using a thermogravimetric analyzer (TGA, TA instrument Q50, USA). XRD pattern was performed using Rigaku DMAX 2500 ($\lambda = 1.54$ Å) diffractometer. The surface morphology was observed using a scanning electron microscopy (SEM, *S*-4300, Hitachi). Electrical conductivity of the composite pellets was measured via a 4-pin probes resistivity meter (LORESTA-GP).

Finally the obtained PANI/$BaTiO_3$ composite particle was dispersed in silicone oil (kinematic viscosity: 50 cS, density: 0.96 g/mL) by using a sonicator for 1 h to prepare ER fluids with 10 vol % particle volume concentration. ER behaviors were measured by a Couette geometry (Z3-DIN) of a rotational rheometer (Physica MC 120, Stuttgart) equipped with a DC high voltage generator (HVG 5000), and an oil bath (VISTHERM VT 100) for temperature control. The gap size of the Z3-DIN was 1.06 mm and its maximum measured stress was 1141 Pa. An electric field was applied for 3 min to obtain an equilibrium chain-like or colum-

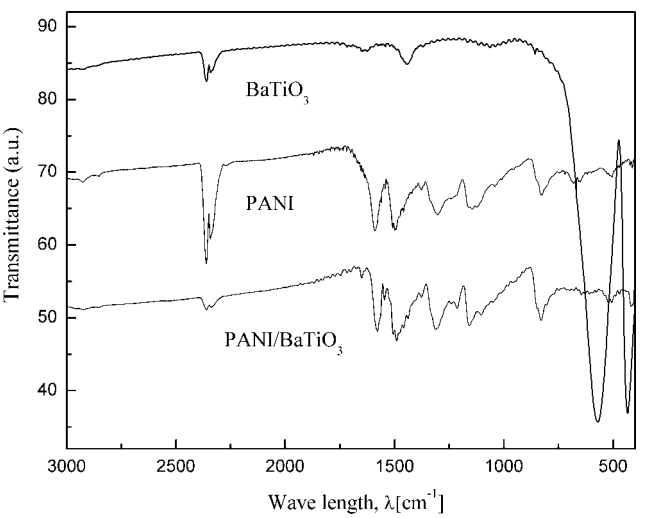

Figure 1 FTIR spectra of PANI, $BaTiO_3$ and PANI/$BaTiO_3$ composite.

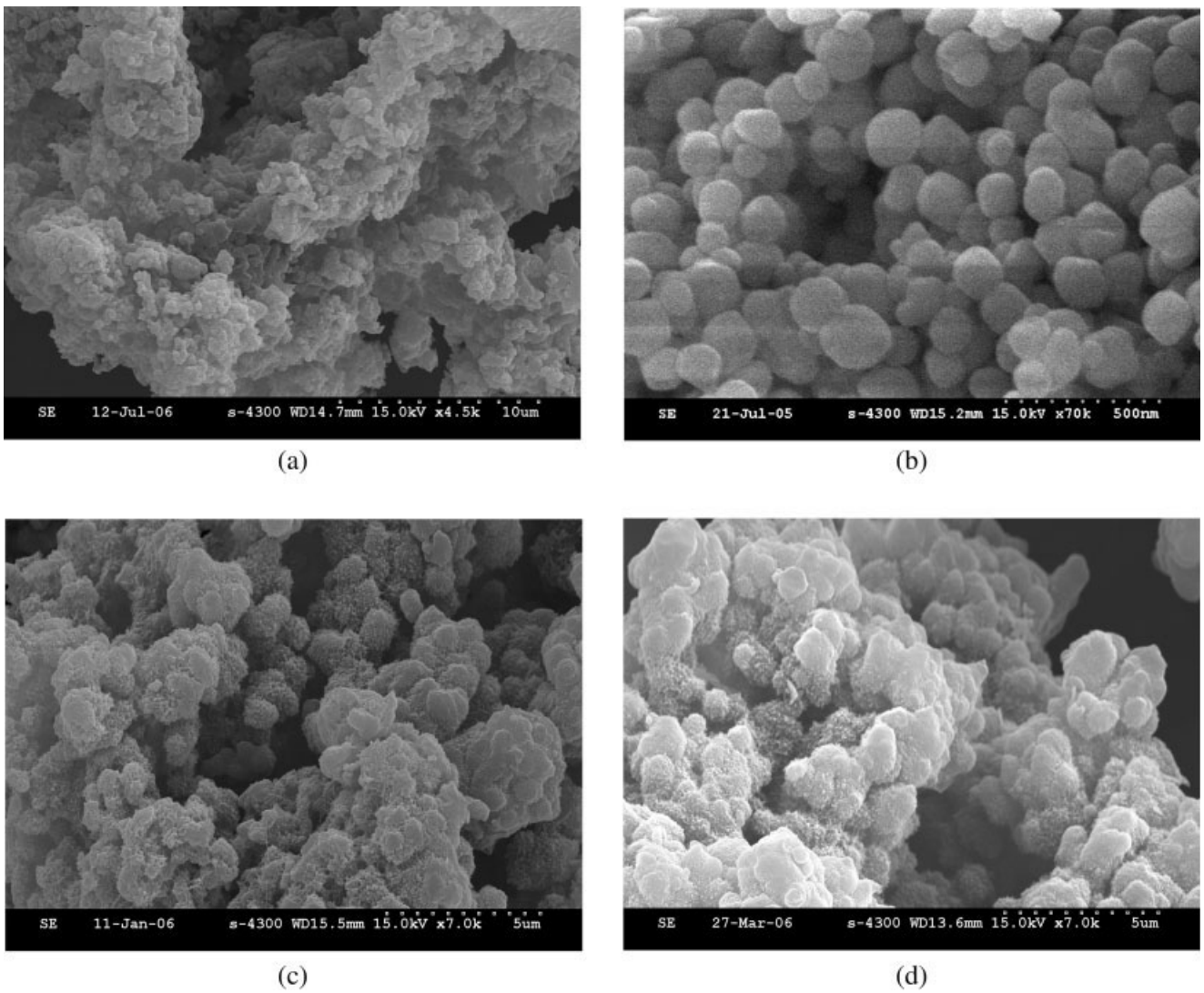

Figure 2 SEM images of pure polyaniline (a), pristine $BaTiO_3$ inorganic nanoparticles (b),PANI/$BaTiO_3$ composite 10 wt % (c) and 25 wt % (d).

nar structure, before applying the shear. All measurements were performed at (25 ± 0.1)°C. To get reproducible and reliable data, the ER fluids were redispersed prior to each experiment, and each measurement was repeatedly carried out at least three times.

Dielectric relaxations of all prepared ER fluids were investigated using the HP 4284A Precision LCR meter with HP 16452A Liquid Test Fixture at room temperature. Frequency of the AC electric fields varied from 20 Hz to 1 MHz, in which the HP 16452A and HP impedance analyzer/LCR meter use the ''capacitive method'' for obtaining relative permittivity by measuring the capacitance of a material sandwiched between parallel electrodes.

RESULTS AND DISCUSSION

Figure 1 represents the FTIR spectra of all three different samples of PANI, $BaTiO_3$, and PANI/$BaTiO_3$ composite. The characteristic peak of PANI at 824 cm^{-1} indicates the out of plane of aromatic C—H. Those other three peaks appeared at 1595, 1496, and 1302 cm^{-1} also attributed to the quinoid unit, benzoid unit, C—N strech of aromatic amine of the PANI, respectively. Distinctive peaks of $BaTiO_3$ appear both in 568 and 438 cm^{-1}. On the basis of these FTIR spectra we can confirm that our organic–inorganic hybrid has been prepared.

On the other hand, it can be noted that previously reported TGA curves for pure PANI, $BaTiO_3$, and PANI/$BaTiO_3$ composite confirmed the composite formation as well as the weight percent of $BaTiO_3$ nanoparticles in the composites.[27]

By observing the SEM images, we find that the inorganic nanoparticles possess a nearly spherical morphology compared with rather big cluster of pure polyaniline (Fig. 2). For the SEM images of the composites, it is apparent that the size of the particles gets bigger than that of the pristine $BaTiO_3$ nanoparticles whose original

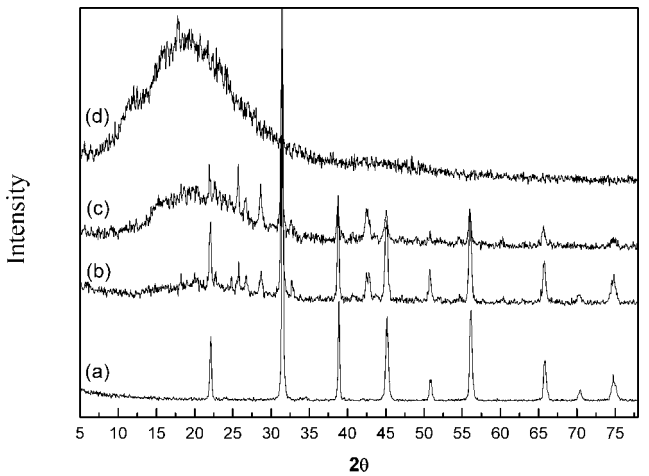

Figure 3 XRD diffraction patterns for pristine $BaTiO_3$ nanoparticles (a), PANI/$BaTiO_3$ composite 25 wt % (b) and 10 wt % (c), pure polyaniline (d).

average size is about 150 nm. This may be interpreted by the successful embedding of inorganic $BaTiO_3$ particles into the PANI polymeric matrix.[31] However, adding much amount of $BaTiO_3$ nanoparticles does not cause much difference in the surface morphology as can be detected from Figure 1(c,d).

Furthermore, examining from the X-ray diffraction patterns represented in Figure 3, we find that pure PANI shows a typical wide amorphous peak at low 2θ region,[32] whereas the pristine $BaTiO_3$ nanoparticles have many distinctive characteristic peaks. As for the PANI/$BaTiO_3$ composites, the intensity of the main peaks characterizing the inorganic structure becomes weakened. This can be attributed to the grown polymer chains which may influence the crystallinity of inorganic $BaTiO_3$ particles as shown in curve (b) and (c) of Figure 3.

The ER behaviors of shear stress versus shear rate of the two types of PANI/$BaTiO_3$ composite (wt % of $BaTiO_3$ to PANI is 10 and 25%) based ER fluids are shown in Figure 4.

The enhancement of shear stress (τ) becomes slightly larger with 25 wt % of $BaTiO_3$ particle within a broad range of shear rate ($\dot{\gamma}$). The typical trends for ER fluids,[33] a decrease of τ with increasing $\dot{\gamma}$ up to a critical shear rate ($\dot{\gamma}_{crit}$), is found. The $\dot{\gamma}_{crit}$ is a transition point of $\dot{\gamma}$ of which the fluid begins to exhibit pseudo-Newtonian behavior (τ increases with $\dot{\gamma}$). In this $\dot{\gamma}$ range, the particle chains appear to be broken by the shear and, further, the particles might have insufficient time to realign themselves along the electric field direction. In a low $\dot{\gamma}$ region, the electrostatic interactions among particles induced by external electric fields are dominant compared to the hydrodynamic interactions induced by the external flow field. The aligned particular structures begin to break with shear deformation, and the broken structures tend to reform the chains by the applied electric field, depending on the magnitude of the applied shear and particle–particle interaction in the fibrils. The decrease in τ is observed when increase in the reformed structures with $\dot{\gamma}$ is not as complete as those before applying shear flow.[34] In other words, as the $\dot{\gamma}$ increases, the destruction rate of the fibrils becomes faster than the reformation rate. It is related to the rate of polarization under the shear by an applied electric field, and will be discussed in conjunction with the dielectric spectra results given below.

Meanwhile, to fit the shear stress curves perfectly, a previously reported De Kee-Turcotte model as well as the CCJ model was adopted. The De Kee-Turcotte model assumes $\tau(\dot{\gamma})$ to be independent of $\dot{\gamma}$ $\dot{\gamma}$ (i.e., $\tau(\dot{\gamma}) = \tau_0$constant) and adopts various expressions for $\eta(\dot{\gamma})$. The common form is:[35]

$$\tau = \tau_o + \eta_1 \dot{\gamma} e^{-t_1 \dot{\gamma}} \quad \text{(De Kee–Turcotte model)} \qquad (1)$$

where t_1 is a time constant having a unit of second. In fitting our data, we adopted the De Kee-Turcotte model.

A suggested model, given below, provides a better fitting of the PANI/$BaTiO_3$ based ER fluids as following:[36]

$$\tau = \frac{\tau_o}{1 + (t_2\dot{\gamma})^{\alpha}} + \eta_\infty \left(1 + \frac{1}{(t_3\dot{\gamma})^{\beta}}\right)\dot{\gamma}. \qquad (2)$$

Here, τ_o is the yield stress defined as the extrapolated stress from low shear rate region, α is related to the decrease in the shear stress, t_2 and t_3 are time constants, and η_∞ is the viscosity at a high shear rate and

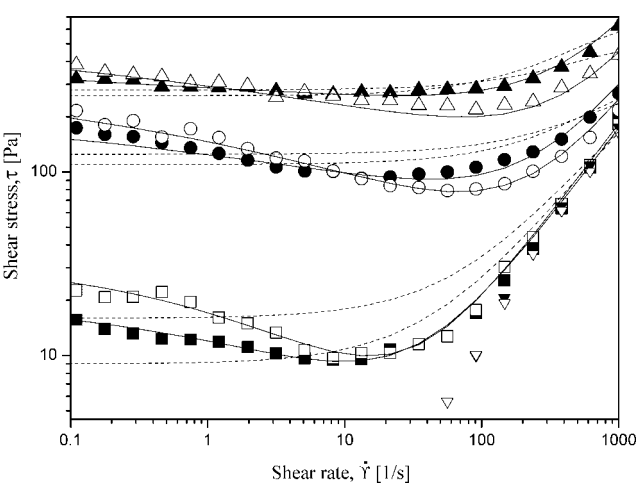

Figure 4 ER curves (shear stress versus shear rate) for PANI/$BaTiO_3$ composites based ER fluids. (▽: 0 kV/mm, □: 0.5 kV/mm, ○: 1.5 kV/mm, △: 2.5 kV/mm. Closed for 10 wt %, open for 25 wt %). The dotted line is from eq. (1).

TABLE I
The Optimal Parameters in Each Model Equation Obtained from the Flow Curve of PANI/$BaTiO_3$ Based ER Fluids

		PANI/$BaTiO_3$ ~10wt %			PANI/$BaTiO_3$ ~25wt %		
Model	Parameters	0.5 (kV/mm)	1.5 (kV/mm)	2.5 (kV/mm)	0.5 (kV/mm)	1.5 (kV/mm)	2.5 (kV/mm)
De Kee-Turcotte	t_0	9	110	260	16	125	280
	h_1	0.18	0.21	0.58	0.19	0.18	0.33
	t_1	0.00015	0.0004	0.00059	0.00023	0.00049	0.00065
CCJ model	t_0	10	120	260	16	150	290
	t_2	0.45	0.9	0.1	0.8	1.2	0.9
	a	0.4	0.2	0.09	0.5	0.3	0.2
	η_∞	0.17	0.25	0.45	0.182	0.217	0.33
	t_3	0.6	0.1	1	10	6	3
	b	0.7	1	2	1	5	1.2

is interpreted as the viscosity in the absence of an electric field. The exponent β has the range $0 < \beta \leq 1$, since $d\tau/d\dot{\gamma} \geq 0$. The yield stresses and the optimal parameters used for these two models in this study are summarized in Table I. We can clearly see that the above six-parameter equation of the CCJ model can cover the stress decrease phenomena at low shear rate region and provide an accurate value for the real yield stress in the case of PANI/$BaTiO_3$ based ER fluids.

For the ER behavior, we can observe that, without an electric field, both the two curves behave like Newtonian behavior with a slope close to 1.0 when exposed to an electric field. The plateau region gets longer when increasing the electric field, which suggests that the electrostatic force gets gradually stronger to resist the hydrodynamic force. Here, the PANI/$BaTiO_3$ composites based ER fluids exhibit better ER effect than that of the pure PANI which may due to the unique ferroelectric properties as well as the high dielectric constant of $BaTiO_3$ nanoparticles.[28] In another work,[29] a $BaTiO_3$ coated-PANI ER system was reported to possesses much polarizable charge in the surface of the coated particles under an external electric field because of the interaction of PANI and $BaTiO_3$, implicating an enhanced polarization strength, consequently lead to a stronger ER behavior.

The ER curves also indicate that the PANI/$BaTiO_3$ (25 wt %) composite based ER fluid shows higher shear stress which may result from much fraction of inorganic $BaTiO_3$ nanoparticles in the composites. To study different behaviors for the two kinds of ER fluids affected by the electric field, we reanalyzed the flow curves. Here, we estimated the dynamic yield stress from a controlled shear rate measurement (CSR) by extrapolating the shear stress at shear rate = 1 s^{-1}.[37] We then plotted the dynamic yield stress as a function of various electric fields. It is well known that in general, the correlation of the dynamic yield stress and electric field was presented as follows:

$$T_y \propto E^m \tag{3}$$

The dependency of the dynamic yield stress on the electric field strength differs from the E^2 dependency suggested by the polarization model depending on the particle concentration,[38,39] particle shape and

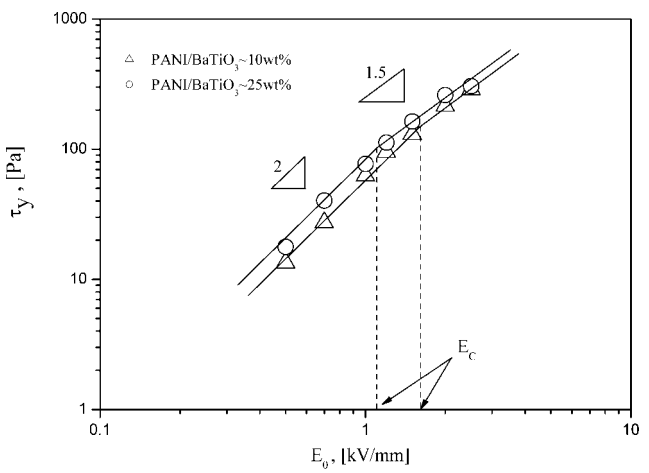

Figure 5 Replotted yield stress versus electric field strengths for PANI/$BaTiO_3$ composites based ER fluids.

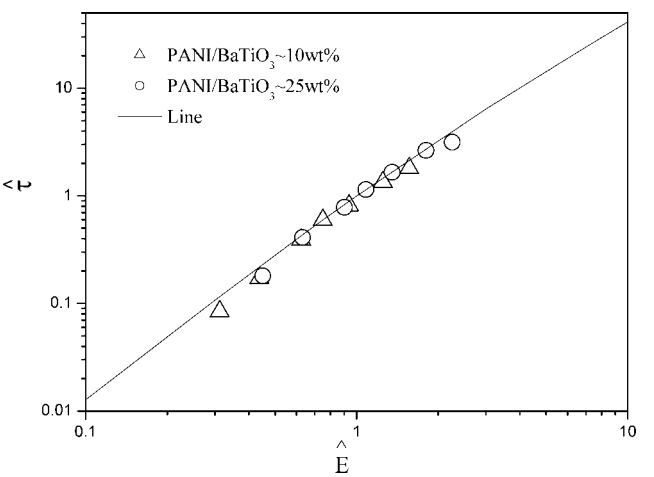

Figure 6 $\hat{\tau}$ versus $\hat{E}$ for PANI/$BaTiO_3$ composites based ER fluids. The solid line is drawn with eq. (5).

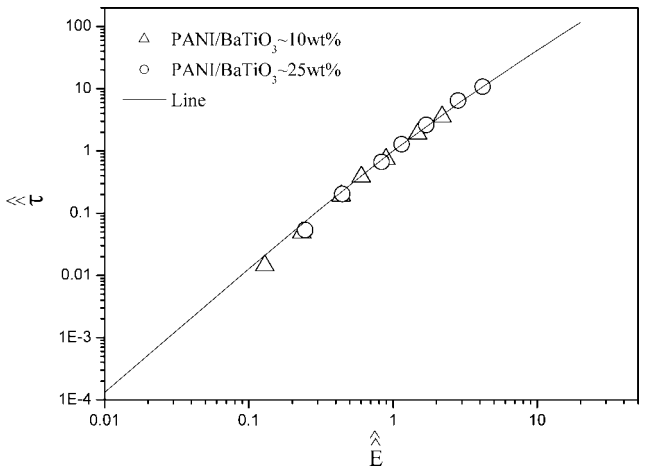

Figure 7 Plot of $\hat{\tau}$ versus $\hat{E}$ for PANI/$BaTiO_3$ composites based ER fluids. The solid line is drawn with eq. (6).

applied electric field strength. The applied electric field induces electrostatic polarized interactions among the particles and also between the particles and the electrodes. However, the polarization model does not describe the flow effect accurately; in that case, the ER response is influenced by the conductivity mismatch and the interaction between particles and medium. Various ER fluids show different exponents in eq. (3). A correlation between yield stress and the electric field strength is represented in Figures 5 and 6. To correlate the dynamic yield stress with the broad range of electric field strengths, Choi et al.[16] introduced the universal yield stress equation

$$\tau_y(E_o) = \alpha E_o^2 \left(\frac{\tanh \sqrt{E_o/E_c}}{\sqrt{E_o/E_c}} \right). \tag{4}$$

Here, the parameter α depends on the dielectric property of the fluid, the particle volume fraction, and the critical electric field, E_c originated from nonlinear conductivity effect can be obtained by the crossover point of the slopes for all ranges of the electric field strengths corresponding to the polarization model (slope = 2) and conductivity model (slope = 1.5), respectively.[40] As shown in Figure 5, the estimated E_c was found to be 1.61 and 1.11 kV/mm for 10 and 25 wt % of PANI/$BaTiO_3$ composites based on ER fluids.

To collapse the data into a single curve, we normalized eq. (4) using E_c and $\tau_y(E_c) = 0.762\alpha E_c^2$

$$\hat{\tau} = 1.313\hat{E}^{3/2} \tanh \sqrt{\hat{E}}. \tag{5}$$

Here, $\hat{E} \equiv E_o/E_c$ and $\hat{\tau} \equiv \tau_y(E_o)/\tau_y(E_c)$. We found that the data obtained from Figure 5 collapsed onto to a single curve via normalized universal yield stress equation [eq. (5)] as shown in Figure 6.

To better fit experimental data, a modified universal correlation introducing an additional parameter b was suggested for the systems that are partly discord with eq. (5) whereas the plots seem to follow an alternative curve.[41] We rescaled $\hat{\tau}$ with $\hat{\hat{\tau}} = \hat{\tau}\hat{E}^{4b}$ and $\hat{E}$ with $\hat{\hat{E}} = \hat{E}^{1+2b}$ for the data, and derived a new equation as

$$\hat{\hat{\tau}} = 1.313\hat{\hat{E}}^{3/2} \tanh \sqrt{\hat{\hat{E}}} \tag{6}$$

for a universal curve. From Figure 7 we were able to confirm that the points $(\hat{\hat{\tau}},\hat{\hat{E}})$, which were recalculated with $b = 0.38$, were located along the curve of eq. (6) with smaller deviations than the points $(\hat{\tau},\hat{E})$ along the curve of eq. (5) in Figure 6. Therefore, eq. (6) is believed to be very useful in constructing the master curve for ER fluids. In addition, note that the deviation of the E_c do not change the scaled universal yield stress equation itself but the point moves following the universal yield stress equation, moving up for the higher E_c and moving down for the lower E_c.[41]

Furthermore, to investigate the ER performances for the two ER fluids in detail, we examined the dielectric properties which may do a favor to interpret the difference in ER effect for the two ER fluids.

Many researchers now prefer to consider the interfacial polymerization as the origin of ER effect. It is well known that the dielectric constant (ε') and loss factor (ε'') are typical results for the interfacial polarization of suspensions including ER fluids which consist of polarizable phases dispersed in insulating media. Lines in Figures 8 and 9 are fitted from the famous Cole–Cole formula eq. (7).[42]

$$\varepsilon^* = \varepsilon' + i\varepsilon'' = \varepsilon_\infty + \frac{\varepsilon_o - \varepsilon_\infty}{1 + (i\omega\lambda)^{1-\alpha}} \tag{7}$$

where the exponent $(1 - \alpha)$ characterizes the broadness of the relaxation time distribution. When $\alpha = 0$,

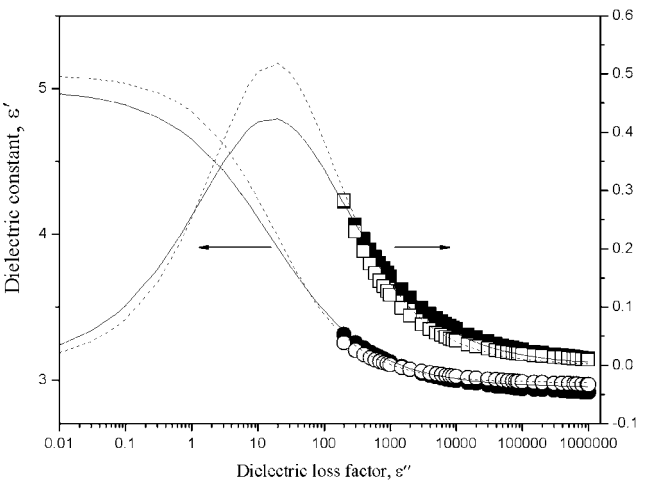

Figure 8 Dielectric spectra of PANI/$BaTiO_3$ composites (closed symbol and solid line for 10 wt %, open symbol and dash line for 25 wt %) based ER fluids.

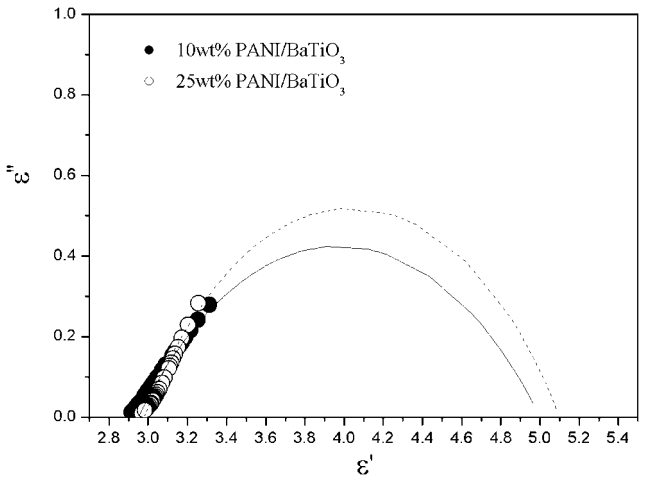

Figure 9 Cole–Cole fitting curves for PANI/$BaTiO_3$ composites (10 and 25 wt %) based ER fluids.

eq. (7) reduces to Debye's well-known single relaxation time model. Here, λ is the relaxation time. Parameters in eq. (7) for the two ER fluids are summarized in Table II.

When analyzing the dielectric spectra, we can see that the relaxation times (λ) are 9.3 and 10 ms for the two ER fluids separately. In general, short relaxation time is known to be related with higher shear stress. Ikazaki et al.[43] has declared that the polarization P responsible for the ER effect can be estimated as follow equation: $P = F\ (\varepsilon'_{brf} - \varepsilon''_{arf}) = F\ (\Delta\varepsilon')$, where F is a function independent of $\Delta\varepsilon'$ and ε'_{brf} and ε''_{arf} are respectively, the dielectric constant below and above the relaxation frequency. On knowing that large polarization will lead to large ER effect, therefore, the value $\Delta\varepsilon'$ also has some positive effect on good ER performance. Hence, in the above table, we can see that the Δε ($\Delta\varepsilon'$) of PANI/$BaTiO_3$ ~10 wt % is a little lower than that of the 25 wt % suggesting a weak ER behavior. In addition, the relaxation times (λ) of PANI/$BaTiO_3$ ~10 wt % is also relative longer which corresponds to a low relaxation frequency. Obviously, the above analysis on the dielectric spectra coincide with the results obtained from comparing the shear stress.

TABLE II
Parameters in Equation 7 for PANI/$BaTiO_3$ Composites (10 wt % and 25 wt %) Based ER Fluids

Parameters	PANI/$BaTiO_3$ ~10 wt %	PANI/$BaTiO_3$ ~25 wt %
ε_0	5	5.10
ε_∞	2.95	2.98
Δε	2.05	2.12
α	0.5	0.42
λ	0.01	0.0093

CONCLUSIONS

A conducting PANI/$BaTiO_3$ composite was synthesized via oxidation polymerization. The physical properties were characterized by FTIR, TGA, SEM, and XRD respectively. A suggested CCJ model was found to describe the ER behaviors more accurately than other reported fitting equations. In addition, to study the different behaviors for the two kinds of ER fluids affected by the electric field, we reanalyzed the flow curves by adopting a universal. At last, an investigated dielectric spectra well interpreted the difference in ER performances caused by the different amount of inorganic $BaTiO_3$ nanoparticles.

References

1. Yoon, D. J.; Kim, Y. D. J Colloid Interface Sci 2006, 303, 573.
2. Zhao, X. P.; Yin, J. B. J Ind Eng Chem 2006, 12, 184.
3. Bossis, G.; Abbo, C.; Cutillas, S.; Lacis, S.; Métayer, C. Int J Mod Phys B 2001, 15, 564.
4. Kim, J. W.; Kim, C. A.; Choi, H. J.; Choi, S. B. Korea-Aust Rheol J 2006, 18, 25.
5. Kuzhir, P.; Bossis, G.; Bashtovoi, V. Int J Mod Phys B 2005, 19, 1229.
6. Carlson, J. D. Int J Mod Phys B 2005, 19, 1463.
7. Sung, J. H.; Park, D. P.; Park, B. J.; Choi, H. J.; Jhon, M. S. Biomacromolecules 2005, 6, 2182.
8. Lu, K. Q.; Shen, R.; Wang, X. Z.; Sun, G.; Wen, W. J.; Liu, J. X. Chin Phys 2006, 15, 2476.
9. Ostubo, Y.; Sekine, M.; Katayama, S. J Colloid Interface Sci 1992, 150, 324.
10. Ko, Y. G.; Choi, U. S. J Appl Polym Sci 2006, 102, 4937.
11. Quadrat, O.; Stejskal, J. J Ind Eng Chem 2006, 12, 352.
12. Gao, Z. W.; Zhao, X. P. Polymer 2004, 45, 1609.
13. Yin, J. B.; Zhao, X. P. Chem Mater 2004, 16, 321.
14. Liu, Y.; Liao, F. H.; Li, J. R.; Zhang, S. H.; Chen, S. M.; Gao, S. Script Mater 2006, 54, 125.
15. Liao, F. H.; Zhang, L.; Li, J. R.; Xu, G.; Li, G. B.; Zhang, S. H.; Gao, S. J Solid State Chem 2003, 176, 273.
16. Choi, H. J.; Cho, M. S.; Kim, J. W.; Kim, C. A.; Jhon, M. S. App Phys Lett 2001, 78, 3806.
17. Wen, W. J.; Huang, X. X.; Yang, S. H.; Lu, K. Q.; Sheng, P. Nat Mater 2003, 2, 727.
18. Hao, T.; Xu, Z.; Xu, Y. J Colloid Interface Sci 1997, 190, 334.
19. Hao, T. Appl Phys Lett 1956, 1997, 70.
20. Yin, J. B.; Zhao, X. P. Chem Phys Lett 2004, 398, 393.
21. Di, K.; Zhu, Y.; Yang, X.; Li, C. J Colloid Interface Sci 2006, 294, 499.
22. Cheng, Q.; He, Y.; Pavlinek, V.; Lengalova, A.; Li, C.; Saha, P. J Mater Sci 2006, 41, 5047.
23. Jun, J. B.; Uhm, S. Y.; Cho, S. H.; Suh, K. D. Langmuir 2004, 20, 2429.
24. Wang, Z.; Shen, R.; Niu, X.; Sun, G.; Lu, K.; Hou, B.; Wen, W. J Phys D: Appl Phys 2005, 38, 1325.
25. Hao, T.; Kawai, A.; Ikazaki, F. Langmuir 1998, 14, 1256.
26. Kim, J. H.; Fang, F. F.; Lee, K. H.; Choi, H. J Korea-Aust Rheol J 2006, 18, 103.
27. Fang, F. F.; Kim, J. H.; Choi, H. J Macromol Symp 2006, 242, 49.
28. Wei, J. H.; Shi, J.; Guan, J. G.; Yuan, R. Z. J Mater Sci 2004, 39, 3457.
29. Wei, J. H.; Shi, J.; Liu, Z. Y.; Guan, J. G.; Yuan, R. Z I.nt J Mod Phys B 2005, 19, 1423.
30. Strounina, E. V.; Shepherd, R.; Kane-Maguire, L. A. P.; Wallace, G. G. Synth Met 2003, 135/136, 289.

31. Li, X.; Chen, W.; Bian, C.; He, J.; Xu, N.; Xue, G. Appl Surface Sci 2003, 217, 16.
32. Deng, J.; He, C.; Peng, Y.; Wang, J.; Long, X.; Li, P.; Chan, A. S. C. Synth Met 2003, 139, 295.
33. Cho, M. S.; Cho, Y. H.; Choi, H. J.; Jhon, M. S. Langmuir 2003, 19, 5875.
34. Kim, J. W.; Liu, F.; Choi, H. J.; Hong, S. H.; Joo, J. Polymer 2003, 44, 289.
35. De Kee, D.; Turcotte, G. Chem Eng Commun 1980, 6, 273.
36. Cho, M. S.; Choi, H. J.; Jhon, M. S. Polymer 2005, 46, 11484.
37. James, D. F.; Blakey, B. C. Korea-Aust Rheol J 2004, 16, 109.
38. Klingerberg, D. J.; van Swol, F.; Zukoski, C. F. J Chem Phys 1991, 94, 6170.
39. See, H. J Ind Eng Chem 2004, 10, 1132.
40. Sung, J. H.; Choi, H. J Korea-Aust Rheol J 2004, 16, 193.
41. Choi, H. J.; Lee, I. S.; Sung, J. H.; Park, B. J.; Jhon, M. S. J Colloid Interface Sci 2006, 295, 291.
42. Lengalova, A.; Pavlinek, V.; Saha, P.; Stejskal, J.; Kitano, T.; Quadrat, O. Physica A 2003, 321, 411.
43. Ikazaki, F.; Kawai, A.; Uchida, K.; Kawakami, T.; Edamura, K.; Sakurai, K.; Anzai, H.; Asako, Y. J Phys D: Appl Phys 1998, 31, 336.